

Ultra-short pulsed laser for nano-texturization associated to plasma immersion implantation for 3D shallow doping:

Application to silicon photovoltaic structures.

M. Halbwx^{*}, T. Sarnet^{*}, Ph. Delaporte^{*}, M. Sentis^{*}
H. Etienne^{**}, F. Torregrosa^{**}, V. Vervisch^{**}, I. Perichaud^{***}, S. Martinuzzi^{***}

^{*}Laboratoire LP3 CNRS UMR 6182 Luminy Marseille, France

^{**}Ion Beam Services IBS, Peynier, France

^{***}Laboratoire TECSSEN CNRS UMR 6122 Marseille, France

ABSTRACT

It has been recently shown (Mazur *et al*) [1-7] that a simple way to improve the photocurrent of a silicon-based solar cell is to irradiate the silicon surface with a series of femtosecond laser pulses, in the presence of a sulfur containing gas. This improves the formation of micro-spikes on the silicon surface that strongly reduces the reflectivity of the illuminated surface for the incident solar light (Black Silicon).

We have prepared photovoltaic structures with different nano-texturization obtained by means of a femtosecond laser, without the use of corrosive gas (under vacuum). To take in account the 3D structured front surface, the emitter doping has been realized by using Plasma Immersion Ion Implantation (so-called PULSION). The results show a photocurrent increase of about 30 % in the laser textured zones.

Keywords: nanotexturization, black silicon, photocurrent, femtosecond laser, plasma immersion doping.

1 INTRODUCTION

In order to increase the efficiency of actual solar cells many different ways are currently being developed by researchers. They include the nano and micro-structuration of the surface [1-8], the use of antireflection (AR) coatings [9], rear totally diffused structures [10], or the use of absorbing nanoparticles [11].

A simple way to improve the silicon-based solar cell efficiency is to irradiate the silicon surface with a series of femtosecond laser pulses, in the presence of a sulfur containing gas [1-7]. This produces micro-spikes on the silicon surface that strongly reduces the incident solar light reflection (Black Silicon). We have in this study created a photovoltaic structure in a silicon wafer, which the illuminated surface was locally nanostructured (squares of 1mm^2) using a femtosecond laser, before the formation of

p-n junction. Various parameters, like polarization, spot size, energy density, number of shots, scanning parameters were chosen to make an appropriate nanotexturization without SF_6 , i.e. the laser treatment was performed under vacuum (10^{-5} mbar).

The p-n junction was obtained by counterdoping the wafer surface by means of the Plasma Immersion Technique (PULSION tool, developed by IBS [11]) followed by Rapid Thermal Annealing (RTA).

It will be shown that the photocurrent increases by 25 to 30 % in the textured areas.

2 EXPERIMENTS

2.1 Processing steps

Samples were n-type silicon doped phosphorus to 10^{15}cm^{-3} (5-20 ohms.cm), cleaned by means of the conventional RCA treatment.

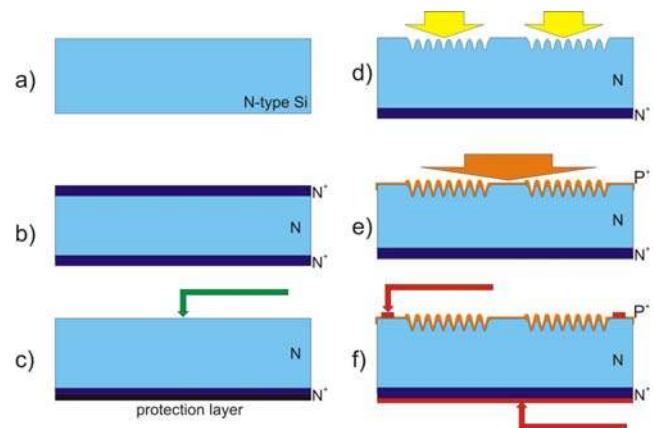


Figure 1: Processing steps of the photocell: a) RCA cleaning, b) creation of n^+ layer by diffusion, c) removal of the front n^+ layer, d) femtosecond laser structuring, e) plasma immersion doping, f) metallization of contacts

The surfaces were first phosphorus diffused from a POCl_3 source in order to create a n^+ layer which helps the formation of a back ohmic contact, while the n^+ front layer was chemically removed (CP_4 etch) before the laser treatment.

After the laser structuring of the surface, the samples have been boron implanted by Plasma Immersion (PULSION, BF_3 , 2 kV, 900°C , 30 mn) and RTA annealed. The junction depth in that case should be about 150 nm, which is much shallower than the 3D laser structures: therefore the junction follows the topography of the structures.

After realizing the p-n junction, the electrical contacts have been deposited by electron gun evaporation: a silver layer on the back side and one aluminum pad on the front non-texturized surface, as shown in Fig. 1. A light-beam induced current LBIC mapping tool is used to detect the increase of the photocurrent in the texturized areas by comparison with the standard surface. This mapping tool was conceived to detect a photocurrent contrast in polycrystalline silicon between defect-containing and defect-free regions, giving rise to electrical image of defects [12]. In our samples it indicates directly if the photocurrent is increased below the nanotexturized areas. The photocurrent produced by a light spot ($\lambda > 800$ nm), 20 μm in diameter, is measured outside and inside the texturized regions, in order to evaluate the enhancement really due to the increase of the light transmission in the wafer bulk.

2.2 Laser Set-up

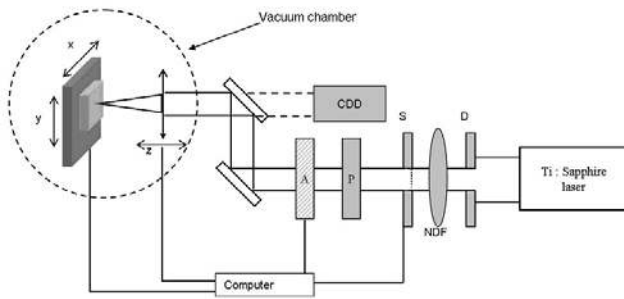


Figure 2: diagram of the femtosecond laser experimental set-up

The engraving of Si (001) was carried out in a vacuum system with a pressure of 5×10^{-5} to 1×10^{-5} mbar. This low pressure considerably reduces the redeposition of unwanted debris from the laser ablation process.

The optical set-up that was used to deliver the laser beam to the sample surface is presented in Figure 2. The micromachining experiments were performed using a Ti:sapphire laser (Hurricane model, Spectra-Physics) at 800 nm, 500 μJ energy, 1 kHz repetition rate and a laser pulse duration of 100 fs. To get a more uniform laser energy distribution, only the center part of the gaussian laser beam

was selected using a square mask (D) of $2 \times 2 \text{ mm}^2$. A spot of about $35 \times 35 \text{ }\mu\text{m}^2$ area was obtained by projecting the mask image onto the sample surface with a planoconvex lens ($f = 50 \text{ mm}$). The laser beam was perpendicular to the sample surface. A computer-controlled XY-stage (for the sample) and Z-stage (for the objective lens) has allowed precise positioning of the spot on the surface sample. The laser energy that was delivered to the sample surface could be attenuated by using a combination of analyzer (A) and polarizer (P) and completed by a set of neutral density filters (NDF). A PC controlled the analyzer rotation, the opening and closing of shutter (S) placed in front of the polarizer, and the XYZ stages. The engraving results are *in situ* monitored by a CCD camera.

Different square surfaces have been irradiated, ranging from $100 \times 100 \text{ }\mu\text{m}^2$ to $1 \times 1 \text{ mm}^2$. The experiment was carried out at two laser fluences: 140 and 185 mJ/cm^2 . The laser-induced structuring of the sample surfaces was produced by scanning a simple straight line (30 μm width) at a speed-velocity of 150 m/s (maximum speed of our stages), with a d shift between the scans to treat the whole surface. The role of beam overlaps on the formed structures was analyzed by varying the distance d between the scans. For each laser fluence, the d value was equal to 1, 2, 5 and 15 μm .

The laser spot displacement was perpendicular to the polarization.

2.3 Experimental Results

Nano and microstructuring of a silicon surface with a pulsed laser (from nanosecond to femtosecond) generally induces the formation of typical wave-like structures (LIPSS, capillary waves, ripples etc...) which have been studied for decades [13].

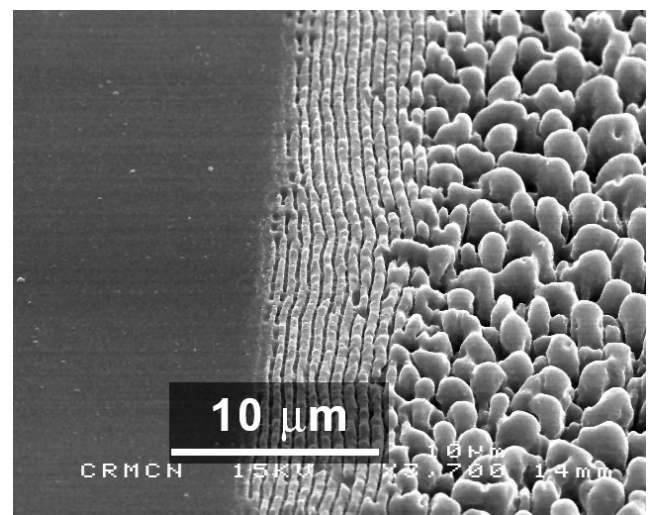


Figure 3: SEM photo of Laser Induced Periodic Surface Structures (LIPSS): capillary waves (periodicity 800 nm, center) and beads (about 2 μm , right)

In this study, the surface topography of these structures was characterized using Scanning Electron Microscopy (SEM) and Optical Microscopy (OM) in dark field mode.

Figure 3 shows different types of structures: the left part is the original Si surface, the center part is formed by capillary waves and the right part features "beads" that are formed with higher number of pulses and energy density. The periodicity of the capillary waves (center) is usually close to the laser wavelength (800 nm), they are formed by the interference between the incident beam and light scattered by minor surface defects. Ablation and melt formation occur at non-uniform depths: after resolidification, the ripple structure is frozen in place and acts as a precursor for the formation of beads, cones and spikes.

For higher energy densities and number of pulses those capillary waves tend to collapse to form a more hydrodynamically stable structure, like the beads observed in Figure 3 (right part). The absorption of light on these beads is not uniform: the ablation is maximized in the valley between the beads which tends to amplify the phenomena and creates more erected structures ("penguin-like" structures), when increasing the energy density and the number of laser pulses.

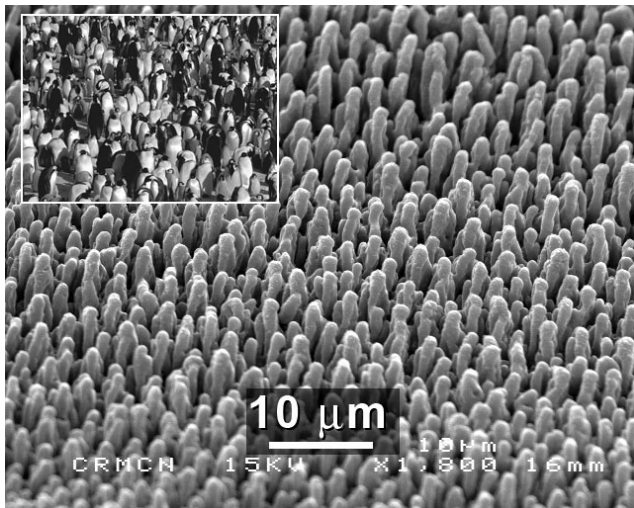


Figure 4: SEM photo of penguin-like structures created by femtosecond laser (top left corner is a picture of a real penguin colony in Antarctica, photo by G. DARGAUD www.gdargaud.net).

Without using SF_6 gas we did not observe spikes, but rather rounded structures, like those shown in Figure 4: these "penguin-like" structures have been named for their similarity with colonies of penguins (*Aptenodytes forsteri*) when they spread over the antarctic ice, standing next to each other.

This type of structure tends to trap the incident light by decreasing the amount of specular (mirror-like) and diffuse reflections. Simple optical simulations have been performed using a commercial ray-tracing renderer (Autodesk 3ds Max) to observe the amount of light reflection on the structured surfaces, using spikes, penguin-like structures and pyramids like the one obtained by KOH anisotropic etching. The best structures seem to be the spikes, immediately followed by the penguin-like structures, in terms of light absorption. The pyramids like the one created by anisotropic etching, which are used nowadays on "high efficient" commercial photocells do not appear to be as absorbant as spikes or penguin-like structures. Moreover, these structures need to be coated (ARC) and are very dependent of the crystal orientation, which is a disadvantage on multi-crystalline silicons, in comparison with the laser structuration which is not sensitive to the different grains orientation.

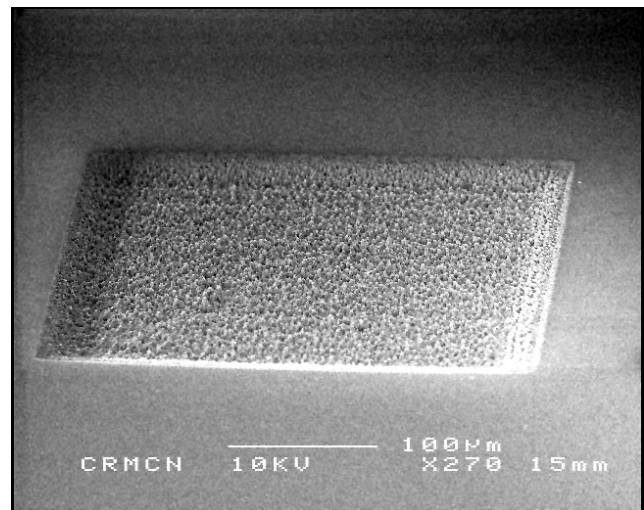


Figure 5: SEM photo of a laser micro-structured area of a photo cell. Size of the treated zone is $300 \mu m^2$, spot size $30 \mu m$, $F= 185 \text{ mJ/cm}^2$, $d=1 \mu m$, scanning speed $v=150 \mu m/s$.

Figure 5 is a general view of a laser structured area (SEM) which shows a good homogeneity of the topography, for $F= 185 \text{ mJ/cm}^2$ and $d=1 \mu m$. When increasing d to higher values ($d>5 \mu m$) the homogeneity is not as good: the lack of overlaps (i.e. number of pulses) tends to create a mixture of capillary waves and beads. Also, working with smaller fluence or number of pulses advantages the formation of capillary waves instead of beads and cones.

The beneficial effect of the texturizations is demonstrated by the LBIC scan maps in Figure 6, which shows that the LBIC signal related to the photocurrent intensity is clearly increased in the laser treated regions.

It is also interesting to notice the high absorption around the laser treated area: this is attributed to the re-deposited

nanoparticles that cover the surroundings of the treated zones.

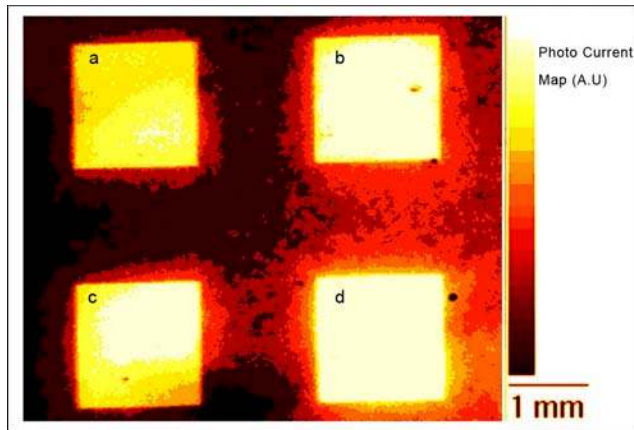


Figure 6: LBIC scan maps showing the increase in the photocurrent in the laser treated zones. spot size $30\ \mu\text{m}$, $v=150\ \mu\text{m/s}$, a) $F=140\ \text{mJ/cm}^2$ $d=1\ \mu\text{m}$, b) $F=140\ \text{mJ/cm}^2$ $d=2\ \mu\text{m}$, c) $F=185\ \text{mJ/cm}^2$ $d=1\ \mu\text{m}$, $F=185\ \text{mJ/cm}^2$, $d=2\ \mu\text{m}$

These nanoparticles were measured by SEM: they range in size from 10 to 100 nm, they are also clearly visible using dark field optical microscopy (Fig. 7).

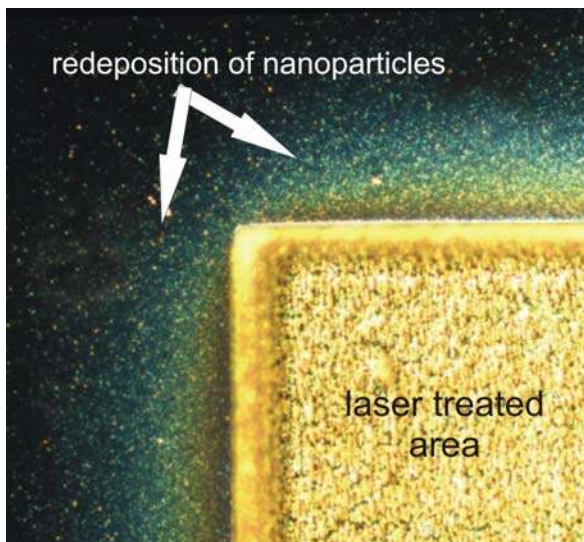


Figure 7: Optical microscope view (Dark Field) of a laser treated area showing the nanoparticle redeposition outside the spot. $F=185\ \text{mJ/cm}^2$, $v=150\ \mu\text{m/s}$.

We measured an average photocurrent outside the spots in the order of 15 nA and smaller, whereas the current in the treated zones is in the range 19 to 21 nA: this implies an improvement in the photocurrent of at least 25 to 30 %. This improvement is probably even better because the photocurrent measured outside the spots have been overestimated by the nanoparticle-increased absorption. The real photocurrent of the non-laser treated surface

should be smaller ($\ll 15\ \text{nA}$) and therefore the gain higher than 30 %. Additional measurements are still in progress and will give better quantitative results.

3 CONCLUSIONS

We have prepared laser-microtexturized Si structures which reduce the reflection of a silicon surface. $1\ \text{mm}^2$ areas were structured on n-type silicon with a femtosecond laser, under vacuum. The boron doped p+ regions were obtained using a Plasma Ion Immersion technique. An increase in the photocurrent was detected by LBIC and reaches more than 30 % in the treated zones.

Notice that this study has been done in a framework of renewable energy and sustainable development promotion: therefore it was important not to use SF_6 which has been identified by the Kyoto Protocol as one of the main greenhouse gas that contribute to climate change and global warming.

REFERENCES

- [1] C. H. Crouch, J. E. Carey, J. M. Warrender, M. J. Aziz, and E. Mazur, *Appl. Phys. Lett.* 84, 1850, 2004.
- [2] M. Y. Shen, C. H. Crouch, J. E. Carey, and E. Mazur, *Appl. Phys. Lett.* 85, 5694, 2004.
- [3] J. E. Carey, C. H. Crouch, M. Shen, and E. Mazur, *Opt. Lett.* 30, 1773, 2005.
- [4] J. E. Carey, Ph.D. dissertation, Harvard Univ., 2004.
- [5] C. H. Crouch, J. Carey, M. Shen, E. Mazur, and F. Y. Genin, *Appl. Phys. Lett.* 79, 1635 2004.
- [6] R. J. Younkin, J. E. Carey, E. Mazur, J. A. Levinson, and C. M. Friend, *J. Appl. Phys.* 93, 2626, 2003.
- [7] B. R. Tull, J. E. Carey, E. Mazur, J. P. McDonald, and S. M. Yalisove "Silicon Surface Morphologies after Femtosecond Laser Irradiation" *MRS Bulletin*, Vol. 31, 626-633 2006
- [8] J. Zhao and A. Wang, *Appl. Phys. Lett.* **88**, 242102, 2006
- [9] A.E Mann, "Optical Coatings For Solar Cells", Spectrolab Sylmar Calif. Report AD0271358, 1960
- [10] M Law et al., "Nanowire dye-sensitized solar cells" *Nature Materials* 4:455-459, 2005
- [11] F.Torregrosa, H.Etienne, G.Matthieu, L.Roux, Proceedings of the 16th International Conference on Ion implantation Technology. AIP conference pp609-613, 2006
- [12] M. Stemmer, *Appl. Surf. Sci.*, 63, 213, 1993.
- [13] M. Birnbaum, "Semiconductor Surface Damage Produced by Ruby Lasers" *Journal of Applied Physics*, 36, 3688, 1965.